RECENT STUDIES OF GEOMETRIC AND RESISTIVE-WALL IMPEDANCE AT SOLEIL

R. Nagaoka, J.-C. Denard, M.-P. Level, Synchrotron SOLEIL, Gif-sur-Yvette, France

Abstract

Recent works on the impedance study made at SOLEIL are reported. Most of which required a special effort to understand and reduce the beam induced heating of the concerned vacuum chamber components.

INTRODUCTION

Coupling impedance studies are of great importance for SOLEIL not only to avoid beam instability, but also to ensure protection of vacuum chambers from EM fields excited by the beam. While the storage ring is envisaged to be operated in high average current (500 mA) and in high bunch current modes (8×10 mA single bunches), the fact that the electron bunches are short (expected to be less than 20 ps rms), namely their frequency spectra extending typically up to 10 GHz range, renders the beam to interact strongly with the resistive impedance components even if they exist at high frequencies. The previous 3D computations [1] indicate that these resistive components arise from taper, slit and cavity-like structures numerously existing in the machine. Not only but the resistive-wall impedance such as arising from a thin metallic coating on a ceramic chamber is a known potential source of the beam induced heating.

BPM TRAPPED MODES

The impedance of a SOLEIL BPM was studied with GdidL [2] by including the entire feed through structure under the waveguide boundary condition, with which the reflection in the former was optimised simultaneously (Figs. 1 left). The main problem encountered here is a mode strongly trapped between the button and the BPM block around 8 GHz, which is expected to be TE_{110} (Figs. 1 right).

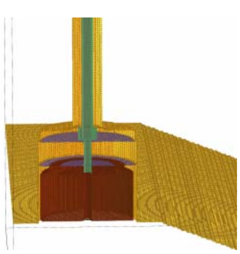

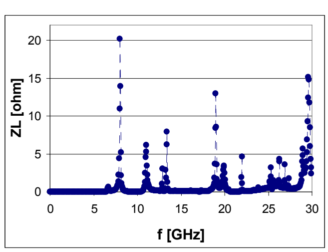

Figures 1: Part of the BPM structure used in GdfidL (left) and the real part of the longitudinal impedance (right).

Trapped modes are troublesome for SOLEIL, since on top of their enhanced sensitivity due to the reduced vertical aperture, short bunches interact with them, as mentioned previously. The dependence of the loss factor on the gap between a button and a BPM block, the button diameter as well as the thickness was followed. A simple solution of reducing the button diameter to raise the trapped mode frequency was not adopted as it is in conflict with the button sensitivity which scales as the square of the diameter. The button thickness was therefore sought to increase, finding that a change from 2 to 5 millimetres reduces the loss factor by as much as a factor of 2 (Fig. 2).

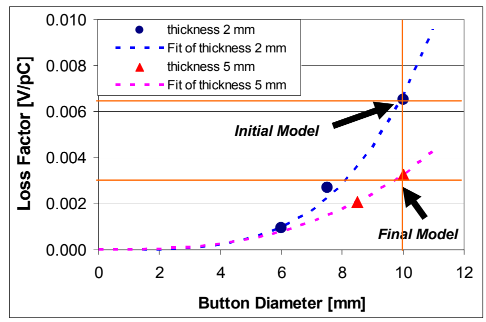

Figure 2: Calculated loss factor versus button diameter for different button thickness.

In view of the risk of spoiling the BPM accuracy due to dilation of the button, the heat that goes into the button was evaluated with the surface integral

$$\iint \frac{H_{//}^2}{2\kappa\delta}\, dF \quad [\mathrm{W}] \tag{1}$$

where $H_{//}$ is the tangential magnetic field obtained in the wake potential calculation, κ is the conductivity and δ is the skin depth at the trapped mode frequency. By assuming in one case that the BPM block is superconducting, a half of the Joule loss was concluded to arise from the button, signifying the power on the button to be around 0.6 W at 500 mA. The study was extended to include a coupled-bunch effect on the loss factor, which may increase the net beam power experienced by an electrode. The effective damping time of the trapped mode was estimated by equating the wall energy loss (Eq. 1) integrated over time to the single bunch energy loss, finding it to be roughly three RF periods. The generalised loss factor was then evaluated by taking into account the passage of subsequent bunches, with a formula

$$k_{loss} = \frac{1}{\pi}\sum_{m=0}^{\infty}\int_0^{\infty} \mathrm{Re}\, Z_{//}(\omega)\cdot e^{-\sigma_\tau^2\omega^2}\cos(m\Delta T\omega)\, d\omega\,, \tag{2}$$

in which ΔT denotes the RF period the trapped mode impedance is fitted with a resonator with its Q-value adjusted to the damping time found. The latter resulted in an enhanced power per electrode of 2.1 W against the original 0.6 W, in the worst case when the trapped mode is in resonance with the RF. To prevent this, gold coating the electrode was pursued, where the power would be reduced down to 0.9 W despite an increased damping time. The idea was however abandoned due to technical complications in realisation, as well as to low probability estimated for the resonance to occur, under the assumption that the trapped mode frequency (fractional part) is random. On the contrary, the probability that the coupled bunch effect reduces the original loss factor was estimated to be higher than 70%.

Table 1: Beam induced heating with a coupled bunch effect, in comparison with the single bunch case. The last column indicates the current dependence of the reading.

Material Block/ button	Q	k_{loss} ratio	P_{tot} [W]	P_{button} [W]	T_{button} [°C]	Curr. dep. [µm]
S.S/S.S	211	3.43	4.18	2.09	180	4.1
S.S/Gold	366	5.45	6.65	0.89	88	1.7
S.S/S.S	Low	1.00	1.22	0.61	68	1.2

TITANIUM COATED CERAMIC CHAMBERS

To evaluate the heating of titanium coated ceramic chambers used for kickers and shakers, their longitudinal impedance was studied analytically. The EM field matching made earlier to chambers having different metallic layers was extended to include dielectric materials in the MKSA unit, working with (E, H). The obtained impedance per unit length for a circular chamber of radius b reads

$$\frac{Z_{//}(\omega)}{L}=\frac{-i}{2\pi\varepsilon_0 cb}\left\{\left(\frac{a}{k}-\frac{k}{a}\right)\cdot\frac{[1+A\tanh(ad)]}{[A+\tanh(ad)]}-\frac{kb}{2}\right\}^{-1} \quad (3)$$

where k=ω/c, a=[1-i·sgn(ω)]/d_s (d_s: skin depth), d the titanium coating thickness, A is equal to $A_0 \equiv i(a/k-k/a)\sqrt{\mu_r\varepsilon_r-1}/\varepsilon_r$ for infinitely thick ceramic, or to $-iA_0\tan(\nu d_c)$ when the thickness is d_c, with $\nu=k\sqrt{\mu_r\varepsilon_r-1}$. Other symbols have their usual meanings. The derived impedance formula comprises that of Piwinski found in Ref. 3. As compared to the impedance of a chamber made of titanium alone, that given by Eq. 3 is characterised by an enhanced real part and a reduced imaginary part. The beam induced power for the case considered (b=12.5 mm and d = 2 µm) turns out to be 46 W for 500 mA uniformly filled beam (σ_L=14 ps) and 43 W for 80 mA beam composed of 8 bunches (σ_L=20 ps), respectively per unit length. These values are found to agree well in the range d=1~5 µm with those obtained from the scheme by S. Milton et al. in Ref. 4, which evaluates the Joule energy of the image charge flowing uniformly across the titanium cross section. The picture assumed in the latter was assessed with the derived EM fields inside the chamber wall. Firstly with the resistivity 50×10^{-8} Ωm of titanium, the skin depth is found to exceed 2 µm up to 30 GHz. This however is only a necessary condition for the image charge to flow uniformly. Since the image current is proportional to the longitudinal electric field E_z in the metal, its radial dependence was followed at as a function of frequency, in comparison with when the titanium thickness is infinite or ceramic is replaced by air. We clearly observe that the longer will be the skin depth as compared to the coating thickness, the more will ceramic render the image current to flow uniformly across titanium (Figs. 3). Such compression of the EM field in the coating due to the presence of ceramic was already pointed out by Piwinski in Ref. 5.

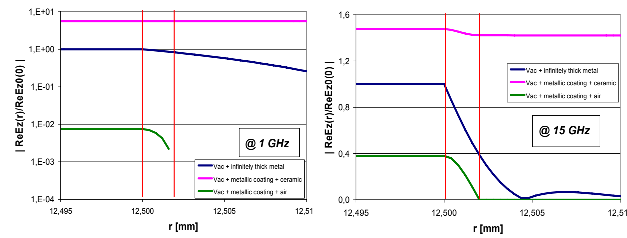

Figures 3: Amplitude of $E_z(r)$ at 1 GHz (left) and 15 GHz (right). Magenta: Ti+ceramic. Blue: Infinite Ti. Green: Ti+air. Red lines: Location of the titanium coating.

We have evaluated the total power for the racetrack shaped SOLEIL ceramic chamber with a circular chamber having the radius equal to the vertical half gap of b=12.5 mm, whose equality is justified by Yokoya [6] and Piwinski [7]. The surface power density, which is more directly related to the temperature distribution, however, shall clearly vary along the perimeter. To derive the latter, Piwinski's study on a flat chamber was utilised, where EM fields are solved analytically in the transverse plane [7]. Although the study assumes an infinitely thick wall, we consider that the geometric effect, such as the dependence of the surface power density on the horizontal position, will not be different for our ceramic chamber with a metallic coating. Justification of applying the flat chamber result to our racetrack chamber will be made later. Integrating E_z over its momentum and frequency variables in the metal and taking its square, the surface power density $P_s(x)$ reads

$$P_s(x)=\frac{\pi^2}{4\cosh^2(\frac{\pi}{2b}x)}\cdot(P_s)_{circle} \quad (4)$$

where $(P_s)_{circle}$ denotes the surface power density of a circular chamber of radius b. The obtained relation indicates that with the vertical half gap of 12.5 mm, the surface density is peaked above and below the beam position (x=0) at nearly 2.5 times the circular chamber value, which decays to zero before x=±20 mm. Since the flat section of the SOLEIL chamber extends to x=±27.5 mm, the use of the flat chamber model may be justified. The derived surface density was used to compute the temperature distribution of the ceramic chambers with a 3D code, by simulating the actual air cooled structure [8]. First results indicated that while with 0.5 µm thick coating, the hottest point is limited to ~90° C at 500 mA, the temperature rises up to ~195° C for 0.2 µm thickness, rendering the latter to be unacceptable [9].

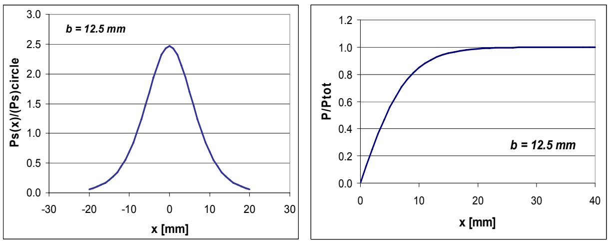

Figures 4: Local surface power density (left) and its integral as a function of the horizontal position *x* (right).

VERTICAL SCRAPER

The geometric impedance of the ESRF type vertical scraper adjusted to SOLEIL was estimated with GdfidL with a major concern on the heating. The impedance was expectedly dominated by the cavity-like structure created at the open position at both ends of the blades (full gap = 25 mm), and by the taper of the blades at the working position (full gap = 8 mm) (Figs. 5 left).

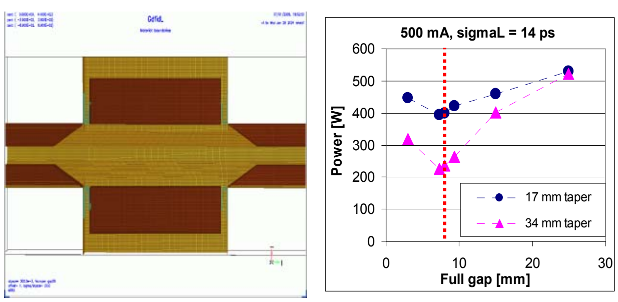

Figures 5: Inverted scraper structure at gap = 8 mm used for the wake potential computation (left) and the beam-induced power versus scraper gap (right).

The beam power turned out to be larger in 500 mA multibunch (σ=14 ps) than in 8×10 mA single bunches (σ=20 ps), which were respectively 530 and 400 W at the open and working positions. These values being excessive above all at the open position, it was decided to reinforce the cooling as well as to inhibit the gap opening beyond 15 mm with high current beam. With the constraint of fixing the total length, doubling of the taper length was attempted with no success, as a significant reduction only occurred around the working position. Reflecting the optimised geometry, the impedance showed a minimum around the working position, where the power changes by less than 5% against ±1 mm gap variations (Figs. 5 right).

STRIPLINE

The impedance of a stripline having four electrodes with transmission lines in one end and short circuited in the other end (Figs.6 left) developed for the tune measurement in the two transverse planes, was investigated. The stripline has a thin slit (0.3 mm) azimuthally along the chamber perimeter, perpendicular to the beam direction at the transmission line position. The impedance consequently exhibits narrow band resonances at relatively low frequencies up to about 5 GHz (Figs.6 right). The overall magnitude of the impedance remains however in the tolerated range ($|Z_{//}/n|_{eff}$ = 0.27 mΩ and the loss factor = 6.7×10^{-3} V/pC).

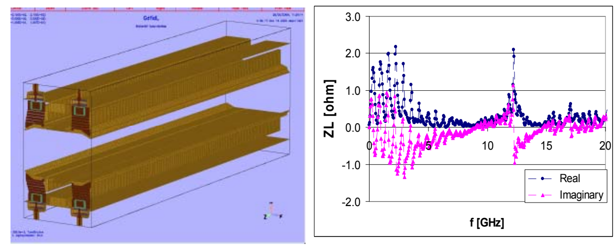

Figures 6: Stripline for the tune measurement (left) and its longitudinal impedance calculated (right).

CONCLUSION

As anticipated, the beam induced heating turned out to be critical for some of the vacuum components of the SOLEIL ring. For precise evaluation of the geometric impedance as well as optimisation of the component design, a detailed 3D computation with fine meshing was essentially important. Likewise, good knowledge of the EM field distribution inside the ceramic chamber obtained on the basis of Piwinski's formulation allowed us to make a realistic evaluation of the local temperature distribution.

ACKNOWLEDGEMENT

The authors thank L. Cassinari, P. Lebasque, J.-P. Daguerre and C. Mariette for their support on this work. One of us (RN) thanks W. Bruns (GdfidL) and Ph. Martinez for their help in the impedance calculations.

REFERENCES

[1] R. Nagaoka, "Numerical Evaluation of Geometric Impedance for SOLEIL", EPAC04, Lucern, p. 2041.
[2] W. Bruns, "The GdfidL Electromagnetic Field Simulator", http://www.gdfidl.de.
[3] Handbook on Accelerator Physics and Engineering, edited by A.W. Chao and M. Tigner, World Scientific.
[4] S. Milton and D. Warner, "The APS Ceramic Chambers", EPAC 1994, London, p. 2494.
[5] A. Piwinski, "Penetration of the Field of a Bunched Beam through a Ceramic Chamber with Metallic Coating", PAC 1977, Chicago.
[6] K. Yokoya, Part. Acc., **41** (1993) 221.
[7] A. Piwinski, "Wake Fields and Ohmic Losses in Flat Vacuum Chambers", DESY HERA 92-04.
[8] J.-P. Daguerre, private communication, Synchrotron SOLEIL.
[9] P. Lebasque et al., "Optimisation of the Coating Thickness on the Ceramic Vacuum Chambers of SOLEIL Storage Ring", in this conference.